Modeling the effects of parathyroid hormone and vitamin D on calcium homeostasis

Inthira Chaiya, Chontita Rattanakul, Sahattaya Rattanamongkonkul, Wannapa Panitsupakamon,

and Sittipong Ruktamatakul

Abstract**—**Calcium homeostasis is an important mechanism in human being. The disorder of such mechanism may leads to serious diseases. In this paper, we propose a mathematical model to describe calcium homeostasis based on the effects of two major factors, parathyroid hormone and vitamin D. The various kinds of dynamics behavior are investigated both theoretically and numerically.

Keywords**—**Calcium homeostasis, geometric singular perturbation, parathyroid hormone, vitamin D.

I. Introduction

In order that all cells in human body function normally, appropriate amounts of calcium ion in the extracellular fluid are required [1]-[4]. The mechanism that maintains the calcium level in the normal range is calcium homeostasis. Two major factors involve in the mechanism are parathyroid hormone and vitamin D [1]-[4].

Parathyroid hormone (PTH) is released from the parathyroid glands in response to the low level of calcium ion in blood [1], [5]. The target organs of PTH are bone, intestine and kidney. On bone, PTH increases the osteoclastic activity resulting in the increase of calcium ion released into blood [1]. On intestine, PTH stimulates the enzyme that converts vitamin D to its active form and then increases calcium absorption from diet [1]. On kidney, PTH stimulates the reabsorption of calcium from urine [1]. Therefore, the increase in PTH level leads to the increase in the calcium level in blood. When the calcium level in blood is high the release of PTH will be decreased in order to maintain the normal range of calcium level in blood.

Vitamin D is produced in human body, requiring only exposure to sunlight. The major biological active metabolite of the vitamin D sterol family is 1,25$(OH)_2D_3$ [3]. After vitamin D is synthesized into its active form, it binds to vitamin D receptor (VDR) located on the target cells [6]. Vitamin D plays important roles in maintaining of calcium balance by enhancing calcium absorption in the intestines and increasing calcium mobilization from bone [6]-[10].

Calcium is very essential for human being. It controls various processes such as the division of cells, the clotting of blood and the contraction of muscles [1]-[4]. The imbalance of calcium level may leads to some diseases such as hypocalcaemia and hypocalcaemia [1]-[4]. Therefore, it is necessary to maintain calcium level within the normal range. In the next section, we then propose a system of nonlinear ordinary differential equations to describe the effects of parathyroid hormone and vitamin D on calcium homeostasis.

II. Model Equations

We propose the following system of ordinary differential equations to describe calcium homeostasis based upon the effects of parathyroid hormone and vitamin D:

$$\frac{dX}{dt} = \frac{a_1}{(k_1+Y)(k_2+Z)} - b_1 X \tag{1}$$

$$\frac{dY}{dt} = \frac{(a_2+a_3X)(a_4-a_5Y)Y}{(k_3+X^2)(k_4+Z)} - b_2 Y \tag{2}$$

$$\frac{dZ}{dt} = \frac{(a_6+a_7X)(a_8+a_9Y)}{(k_5+X)(k_6+Y)} - b_3 Z \tag{3}$$

where $X(t)$ denotes the concentration of parathyroid hormone (PTH) above the basal level in blood at time t, $Y(t)$ denotes the concentration of calcitriol (the active form of vitamin D) in blood at time t, and $Z(t)$ denotes the concentration of calcium in blood at time t.

Equation (1) represents the rate of change of the concentration of PTH above the basal level in blood at time t. The first term on the right hand side stands for the secretion

This work was supported by the Centre of Excellence in Mathematics, Commission on Higher Education, Thailand and the Royal Golden Jubilee Ph.D. Program (contract number PHD53K0191).

I. Chaiya is with the Department of Mathematics, Faculty of Science, Mahidol University, Thailand and the Centre of Excellence in Mathematics, the Commission on Higher Education, Thailand (e-mail: g5438789@student.mahidol.ac.th).

C. Rattanakul is with the Department of Mathematics, Faculty of Science, Mahidol University, Thailand and the Centre of Excellence in Mathematics, the Commission on Higher Education, Thailand (corresponding author, phone: 662-201-5340; fax: 662-201-5343; e-mail: chontita.rat@mahidol .ac.th).

S. Rattanamongkonkul is with the Department of Mathematics, Faculty of Science, Burapha University, Thailand and the Centre of Excellence in Mathematics, the Commission on Higher Education, Thailand (e-mail: sahattay@buu.ac.th).

W. Panitsupakamon is with the Department of Mathematics, Faculty of Science, Silpakorn University, Thailand and the Centre of Excellence in Mathematics, the Commission on Higher Education, Thailand (e-mail: wannapa@su.ac.th).

S. Ruktamatakul is with the Department of Mathematics, Faculty of Liberal Arts Science, Kasetsart University, Thailand and the Centre of Excellence in Mathematics, the Commission on Higher Education, Thailand (e-mail: faasspr@nontri.ku.ac.th).

rate of PTH from the parathyroid glands in response to the level of calcium and active vitamin D in blood. When the calcium level or vitamin D level is high the secretion rate of PTH will be decreased in order to counter balance the high level of calcium in blood. The last term stands for the removal rate of PTH from the system.

Equation (2) represents the rate of change of the concentration of calcitriol (active vitamin D) in blood at time *t*. The first term on the right hand side stands for the synthesis rate of active vitamin D in response to the level of calcium and PTH in blood. The last term stands for the removal rate of active vitamin D from the system.

Equation (3) represents the rate of change of the concentration of calcium in blood at time *t*. The first term on the right hand side stands for the rate of change in calcium level corresponding to the level of PTH and active vitamin D in blood. The last term stands for the removal rate of calcium from the system.

Note that all parameters in the system are assumed to be positive.

III. GEOMETRIC SINGULAR PERTURBATION ANALYSIS

Assuming that PTH has the fastest dynamics, active vitamin D has the intermediate dynamics and calcium has the slowest dynamics. In order to apply the geometric singular perturbation technique [11], [12] to our system, we then scale the dynamics of the three components and parameters of the system in term of small positive parameters $0<\varepsilon<<1$ and $0<\delta<<1$ as follows. Letting $x=X$, $y=Y$, $z=Z$, $c_1=a_1$, $c_2=\frac{a_2}{\varepsilon}$, $c_3=\frac{a_3}{\varepsilon}$, $c_4=a_4$, $c_5=a_5$, $c_6=\frac{a_6}{\varepsilon\delta}$, $c_7=\frac{a_7}{\varepsilon\delta}$, $c_8=a_8, c_9=a_9$, $d_1=b_1, d_2=\frac{b_2}{\varepsilon}$, $d_3=\frac{b_3}{\varepsilon\delta}$, the system (1)-(3) can be written as:

$$\frac{dx}{dt}=\frac{c_1}{(k_1+y)(k_2+z)}-d_1x \equiv f(x,y,z) \tag{4}$$

$$\frac{dy}{dt}=\varepsilon\left(\frac{(c_2+c_3x)(c_4-c_5y)y}{(k_3+x^2)(k_4+z)}-d_2y\right)\equiv\varepsilon g(x,y,z) \tag{5}$$

$$\frac{dz}{dt}=\varepsilon\delta\left(\frac{(c_6+c_7x)(c_8+c_9y)}{(k_5+x)(k_6+y)}-d_3z\right)\equiv\varepsilon\delta h(x,y,z) \tag{6}$$

The shapes and relative positions of the manifolds $\{f=0\}$, $\{g=0\}$, and $\{h=0\}$ determine the shapes, directions and speeds of the solution trajectories. We then investigate each of the equilibrium manifolds in detail.

The manifold $\{f=0\}$

This manifold is given by the equation

$$x=\frac{c_1}{d_1(k_1+y)(k_2+z)}\equiv A_1(y,z) \tag{7}$$

which intersects the $(x,y)-$ plane along the curve

$$x=\frac{c_1}{d_1k_2(k_1+y)} \tag{8}$$

It intersects the $x-$ axis at the point where

$$x=\frac{c_1}{d_1k_1k_2}\equiv x_1 \tag{9}$$

The manifold $\{f=0\}$ also intersects the $(x,z)-$ plane along the curve

$$x=\frac{c_1}{d_1k_1(k_2+z)} \tag{10}$$

Note that, in the first octant, $x=A_1(y,z)$ is an decreasing function of y and z so that $A_1(y,z)\to 0$ as $y\to\infty$ and $A_1(y,z)\to 0$ as $z\to\infty$.

The manifold $\{g=0\}$

This manifold consists of two sub-manifolds, the trivial manifold $y=0$ and the nontrivial manifold given by the equation

$$y=\frac{c_4}{c_5}-\frac{d_2(k_3+x^2)(k_4+z)}{c_5(c_2+c_3x)}\equiv A_2(x,z) \tag{11}$$

which is a decreasing function of z in the first octant.

The nontrivial manifold intersects the $(x,y)-$ plane along the curve

$$y=\frac{c_4}{c_5}-\frac{d_2k_4(k_3+x^2)}{c_5(c_2+c_3x)}\equiv B_1(x) \tag{12}$$

attaining its maximum at the point where

$$x=\frac{-c_2+\sqrt{c_2^{\,2}+c_3^{\,2}k_3}}{c_3}\equiv x_2 \tag{13}$$

and

$$y=\frac{c_4}{c_5}-\frac{d_2k_4(k_3+x_2^{\,2})}{c_5(c_2+c_3x_2)}\equiv y_2 \tag{14}$$

In addition, $y=B_1(x)$ intersects the $x-$ axis and $y-$ axis at the points where

$$x=\frac{c_3c_4+\sqrt{(c_3c_4)^2+4d_2k_4(c_2c_4-d_2k_3k_4)}}{2d_2k_4}\equiv x_3$$

and $y=\frac{c_2c_4-d_2k_3k_4}{c_2c_5}\equiv y_1$, respectively. Note that $x_3>0$ and $y_1>0$ if

$$c_2c_4>d_2k_3k_4 \tag{15}$$

The nontrivial manifold intersects the $(x,z)-$ plane along the curve

$$z=\frac{1}{d_2}\left[\frac{c_4(c_2+c_3x)}{(k_3+x^2)}-d_2k_4\right]\equiv B_2(x) \tag{16}$$

attaining its maximum at the point where $x=x_2$ and

$$z=\frac{1}{d_2}\left[\frac{c_4(c_2+c_3x_2)}{(k_3+x_2^{\,2})}-d_2k_4\right]\equiv z_2 \tag{17}$$

In addition, $y=B_2(x)$ intersects the $x-$ axis and $z-$ axis at the point where $x=x_3$ and

$$z = \frac{c_2 c_3 - d_2 d_3 k_4}{d_2 k_3} \equiv z_1, \quad (18)$$

respectively. Note that $z_1 > 0$ if the inequality (15) holds.

The nontrivial manifold intersects the $(y,z)-$plane along the line

$$y = \frac{c_2 c_4 - d_2 k_3 k_4}{c_2 c_5} - \frac{d_2 k_3}{c_2 c_5} z = B_3(z) \quad (19)$$

which intersects the $y-$axis and the $z-$axis at the point where $y = y_1$ and $z = z_1$, respectively.

The manifold $\{f = 0\}$ intersects the trivial manifold $y = 0$ of the manifold $\{g = 0\}$ along the curve

$$\left\{ x = \frac{c_1}{d_1 k_1 (k_2 + z)}, y = 0 \right\} \quad (20)$$

which is asymptotic to the line $x = 0$.

The manifold $\{f = 0\}$ intersects the nontrivial manifold $\{g = 0\}$ along the curve

$$\left\{ x = \frac{c_1}{d_1(k_1 + y)(k_2 + z)}, y = \frac{c_4}{c_5} - \frac{d_2(k_3 + x^2)(k_4 + z)}{c_5(c_2 + c_3 x)} \right\} \quad (21)$$

attaining its relative maximum at the point (x_2, y_M, z_M) where y_M is a real solution of

$$Ay^2 + By + C = 0 \quad (22)$$

where

$$A = -c_5 d_1 x_2 (c_2 + x_2) < 0$$

$$B = d_1 d_2 x_2 (k_3 + x_2^2)(k_2 - k_4) + d_1 x_2 (c_2 + c_3 x_2)(c_4 - c_5 k_1)$$

$$C = c_4 d_1 k_1 x_2 (c_2 + c_3 x_2) + d_1 d_2 k_1 x_2 (k_3 + x_2^2)(k_2 - k_4) - c_1 d_2 (k_3 + x_2^2)$$

and

$$z_M = \frac{c_1}{d_1 x_2 (k_1 + y_M)} - k_2 \quad (23)$$

Note that y_M exists in the first octant and is unique if

$$C > 0 \quad (24)$$

Moreover, $z_M > 0$ if

$$y_M < \frac{c_1}{d_1 k_2 x_2} - k_1 \quad (25)$$

provided that $y_M > 0$.

The manifold $\{h = 0\}$

This manifold is given by the equation

$$z = \frac{(c_6 + c_7 x)(c_8 + c_9 y)}{d_3 (k_5 + x)(k_6 + y)} \equiv A_3(x, y) \quad (26)$$

which intersects the $(x,z)-$ plane along the curve

$$z = \frac{c_8 (c_6 + c_7 x)}{d_3 k_6 (k_5 + x)} \equiv B_4(x) \quad (27)$$

It intersects the $z-$ axis at the point where

$$z = \frac{c_6 c_8}{d_3 k_5 k_6} \equiv z_3 \quad (28)$$

and is also asymptotic to the line

$$z = \frac{c_7 c_8}{d_3 k_6} \equiv z_4 \quad (29)$$

The manifold intersects the $(y,z)-$ plane along the curve

$$z = \frac{c_6 (c_8 + c_9 y)}{d_3 k_5 (k_6 + y)} \equiv B_5(y) \quad (30)$$

which intersects the $z-$axis at the point where $z = z_3$ and is also asymptotic to the line

$$z = \frac{c_6 c_9}{d_3 k_5} \equiv z_5 \quad (31)$$

The manifold $\{f = 0\}$ intersects the manifold $\{h = 0\}$ along the curve

$$\left\{ x = \frac{c_1}{d_1 (k_1 + y)(k_2 + z)}, z = \frac{(c_6 + c_7 x)(c_8 + c_9 y)}{d_3 (k_5 + x)(k_6 + y)} \right\} \quad (32)$$

which intersects the trivial manifold $y = 0$ of the manifold $\{g = 0\}$ at the point $S_1 = (x_4, 0, z_6)$ where x_4 is a positive root of

$$Dy^2 + Ey + F = 0 \quad (33)$$

where

$$D = c_7 c_8 d_1 k_1 + d_1 d_3 k_1 k_2 k_6 > 0$$

$$E = c_6 c_8 d_1 k_1 + d_1 d_3 k_1 k_2 k_5 k_6 - c_1 d_3 k_6$$

$$F = -c_1 d_3 k_5 k_6 < 0$$

and

$$z_6 \equiv \frac{c_1}{d_1 k_1 x_4} - k_2 \quad (34)$$

Note that (37) always has a unique positive root x_4 and $z_6 > 0$ if

$$c_1 > k_2 d_1 k_1 x_4 \quad (35)$$

Moreover, the curve $\{f = h = 0\}$ in (35) intersects the nontrivial manifold of $\{g = 0\}$ at the point $S_2 = (x_{S_2}, y_{S_2}, z_{S_2})$ where

$$x_{S_2} = \frac{c_1}{d_1 (k_1 + y_{S_2})(k_2 + z_{S_2})},$$

$$y_{S_2} = \frac{c_4}{c_5} - \frac{d_2 (k_3 + x_{S_2}^2)(k_4 + z_{S_2})}{c_5 (c_2 + c_3 x_{S_2})},$$

$$z_{S_2} = \frac{(c_6 + c_7 x_{S_2})(c_8 + c_9 y_{S_2})}{d_3 (k_5 + x_{S_2})(k_6 + y_{S_2})}$$

Note that $y_{S_2} > 0$ if

$$c_4 (c_2 + c_3 x_{S_2}) > d_2 (k_3 + x_{S_2}^2)(k_4 + z_{S_2}) \quad (36)$$

Case 1 If ε and δ are sufficiently small, and the inequalities (15), (24), (25), (35), (36) hold, and

$$x_2 < x_{S_2} < x_3 < x_4 < x_1 \quad (37)$$

$$z_4 < z_M < z_5 \quad (38)$$

where all parametric values are defined as above, then a periodic solution exists for the system of (4)-(6). The proof of the theorem is based on geometric singular perturbation method [11]-[12].

If all conditions in Case 1 hold, then the shapes of the manifolds $\{f=0\}$, $\{g=0\}$ and $\{h=0\}$ are positioned as in Fig. 1. Starting from a point A in front of the manifold $\{f=0\}$. Here, $\{f<0\}$ and a fast transition will then bring the system to the point B on the manifold $\{f=0\}$ in the direction of decreasing x. Here, $\{g>0\}$ and a transition at intermediate speed will be made in the direction of increasing y until the point C on the curve $\{f=g=0\}$ is reached. A slow transition then follows along this curve to the point D where the stability of sub-manifold will be lost. A jump to point E on the other stable part of $\{f=g=0\}$ followed by a slow transition in the direction of decreasing z until the point F is reached since $\{h<0\}$ here. The stability of sub-manifold will be lost. A jump to point G on the other stable part of $\{f=g=0\}$ followed by a slow transition in the direction of increasing z since $\{h>0\}$ here. Consequently, a slow transition will bring the system back to the point D, followed by flows along the same path repeatedly, resulting in the closed orbit DEFGD. Thus, for sufficiently small ε and δ, a periodic solution of the system exists.

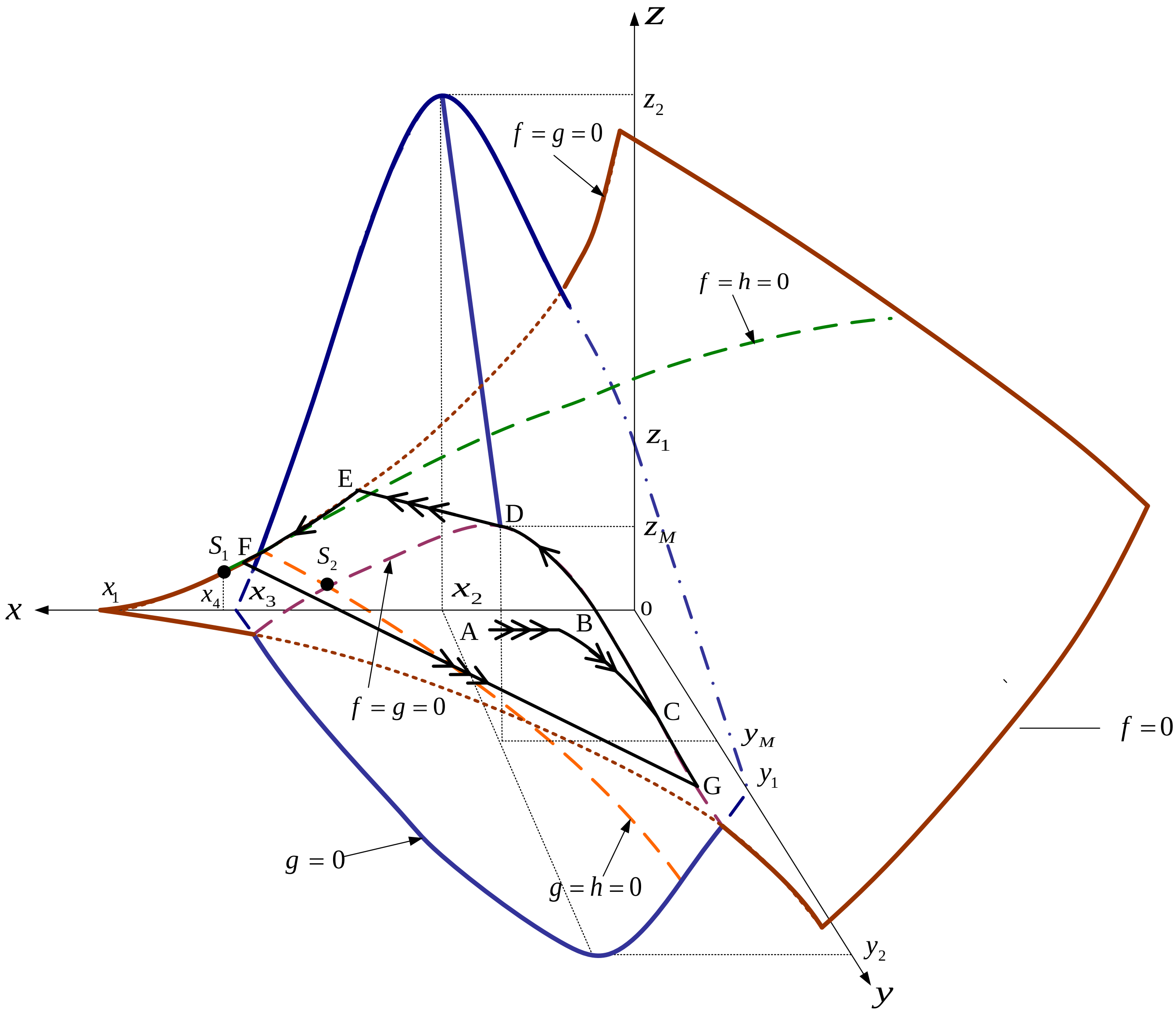

Fig. 1 The three equilibrium manifolds $\{f=0\},\{g=0\}$ and $\{h=0\}$ in $(x,y,z)-$space in Case 1 . Segments of the trajectories with one, two, and three arrows represent slow, intermediate, and fast transitions, respectively.

Case 2 If ε and δ are sufficiently small, and the inequalities (15), (24), (25), (35), (36) hold, and

$$x_{S_2} < x_2 < x_4 < x_3 < x_1 \tag{39}$$

$$z_4 < z_M < z_5 \tag{40}$$

where all parametric values are defined as above, then the manifolds are positioned as in Fig. 2 and the system of (4)-(6) will have a stable equilibrium point.

If all conditions in Case 2 hold, then the shapes of the manifolds $\{f=0\}$, $\{g=0\}$ and $\{h=0\}$ are positioned as in Fig. 2. Starting from a point A in front of the manifold $\{f=0\}$. Here, $\{f<0\}$ and a fast transition will then bring the system to the point B on the manifold $\{f=0\}$ in the direction of decreasing x. Here, $\{g>0\}$ and a transition at intermediate speed will be made in the direction of increasing y until point C on the curve $\{f=g=0\}$ is reached. Here, $\{h>0\}$ and a slow transition then follows along this curve until the point S_2 is reached. Thus, the solution trajectory is expected in this case to tend toward this stable equilibrium point S_2 as time passes.

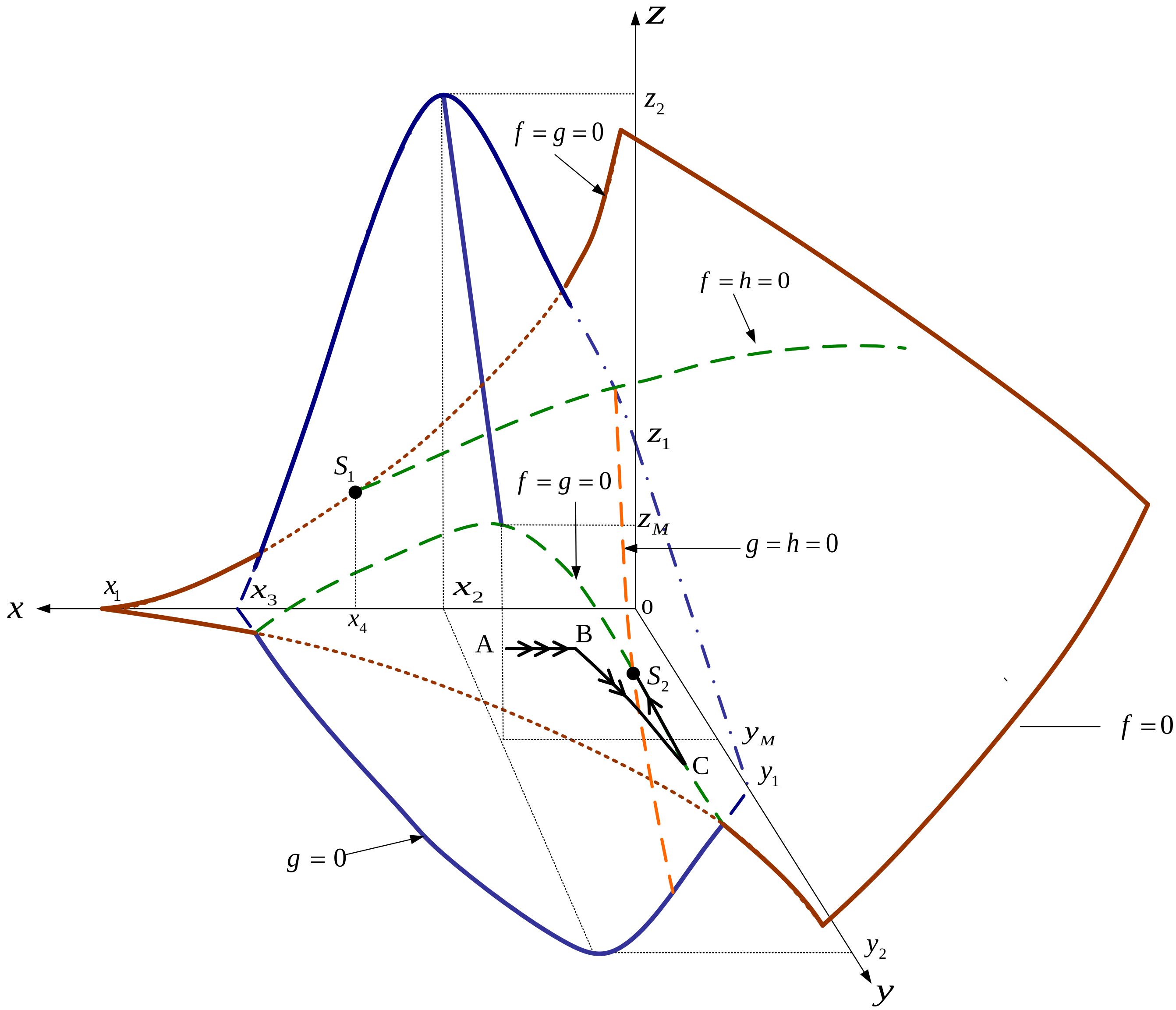

Fig. 2 The three equilibrium manifolds $\{f=0\}$, $\{g=0\}$ and $\{h=0\}$ in (x,y,z) – space in Case 2 . Segments of the trajectories with one, two, and three arrows represent slow, intermediate, and fast transitions, respectively.

Case 3 If ε and δ are sufficiently small, and the inequalities (15), (24), (25), (35), (36) hold, and

$$x_2 < x_{S_2} < x_4 < x_3 < x_1 \quad (41)$$

$$z_4 < z_M < z_5 \quad (42)$$

where all parametric values are defined as above, then the manifolds are positioned as in Fig. 3 and the system of (4)-(6) will have a stable equilibrium point.

If all conditions in Case 3 hold, then the shapes of the manifolds $\{f=0\}$, $\{g=0\}$ and $\{h=0\}$ are positioned as in Fig. 3. Starting from a point A in front of the manifold $\{f=0\}$. Here, $\{f<0\}$ and a fast transition will then bring the system to the point B on the manifold $\{f=0\}$ in the direction of decreasing x. Here, $\{g>0\}$ and a transition at intermediate speed will be made in the direction of increasing y until point C on the curve $\{f=g=0\}$ is reached. Here, $\{h>0\}$ and a slow transition then follows along this curve to the point D where the stability of sub-manifold will be lost. A jump to point E on the other stable part of $\{f=g=0\}$ followed by a slow transition in the direction of decreasing z until the point S_1 is reached since $\{h<0\}$ here. Thus, the solution trajectory is expected in this case to tend toward this stable equilibrium point S_1 as time passes.

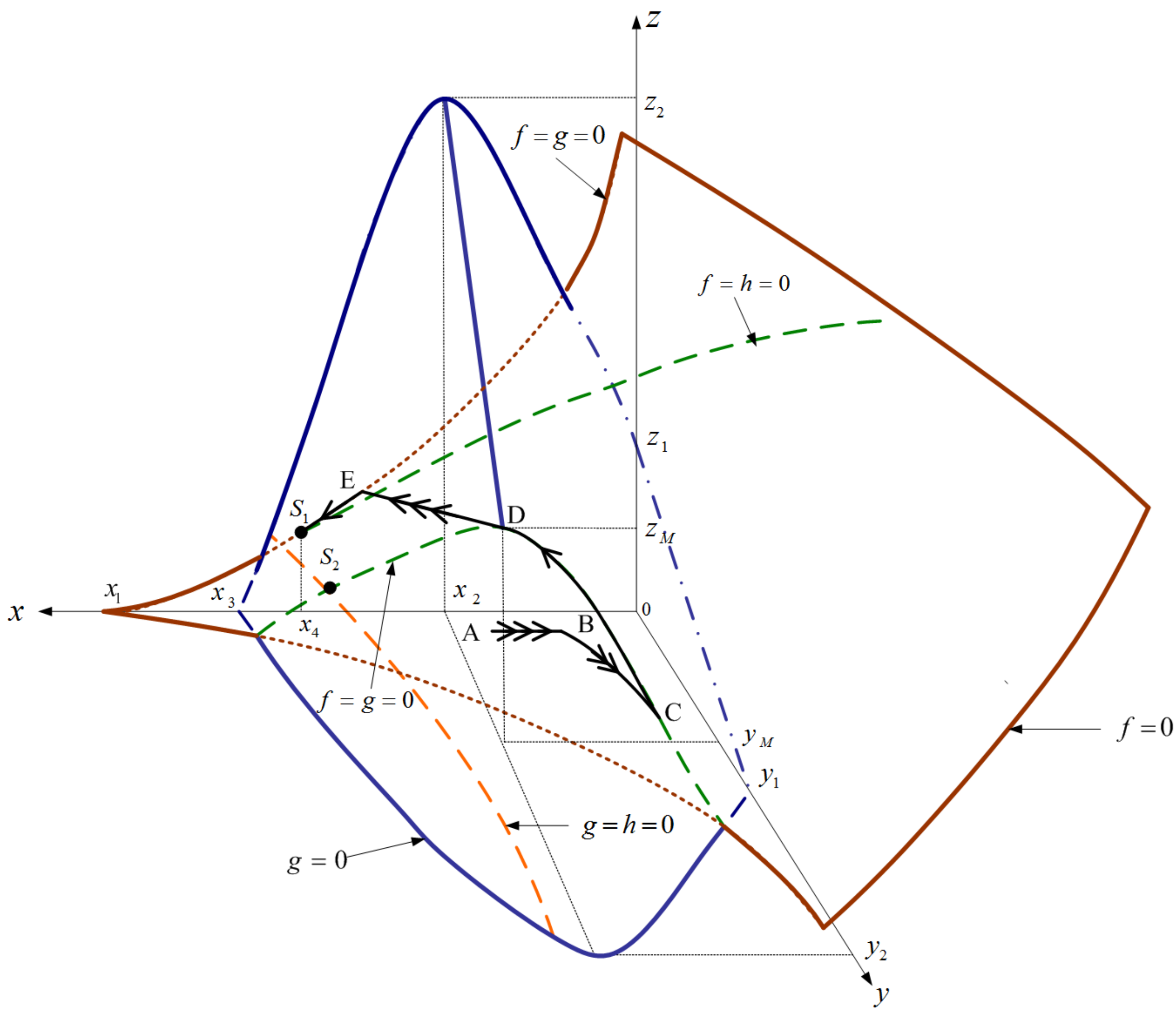

Fig. 3 The three equilibrium manifolds $\{f=0\},\{g=0\}$ and $\{h=0\}$ in $(x,y,z)-$space in Case 3 . Segments of the trajectories with one, two, and three arrows represent slow, intermediate, and fast transitions, respectively.

IV. COMPUTER SIMULATIONS

A numerical result of the system (4)-(6) is presented in Fig. 4, with parametric values chosen to satisfy the inequalities identified in Case 1. The solution trajectory, shown in Fig. 4a project onto the (x, y)-plane, tends to a limit cycle as theoretically predicted. The corresponding time courses of the PTH, active vitamin D, and calcium concentration are as shown in Fig. 4b, 4c, and 4d respectively.

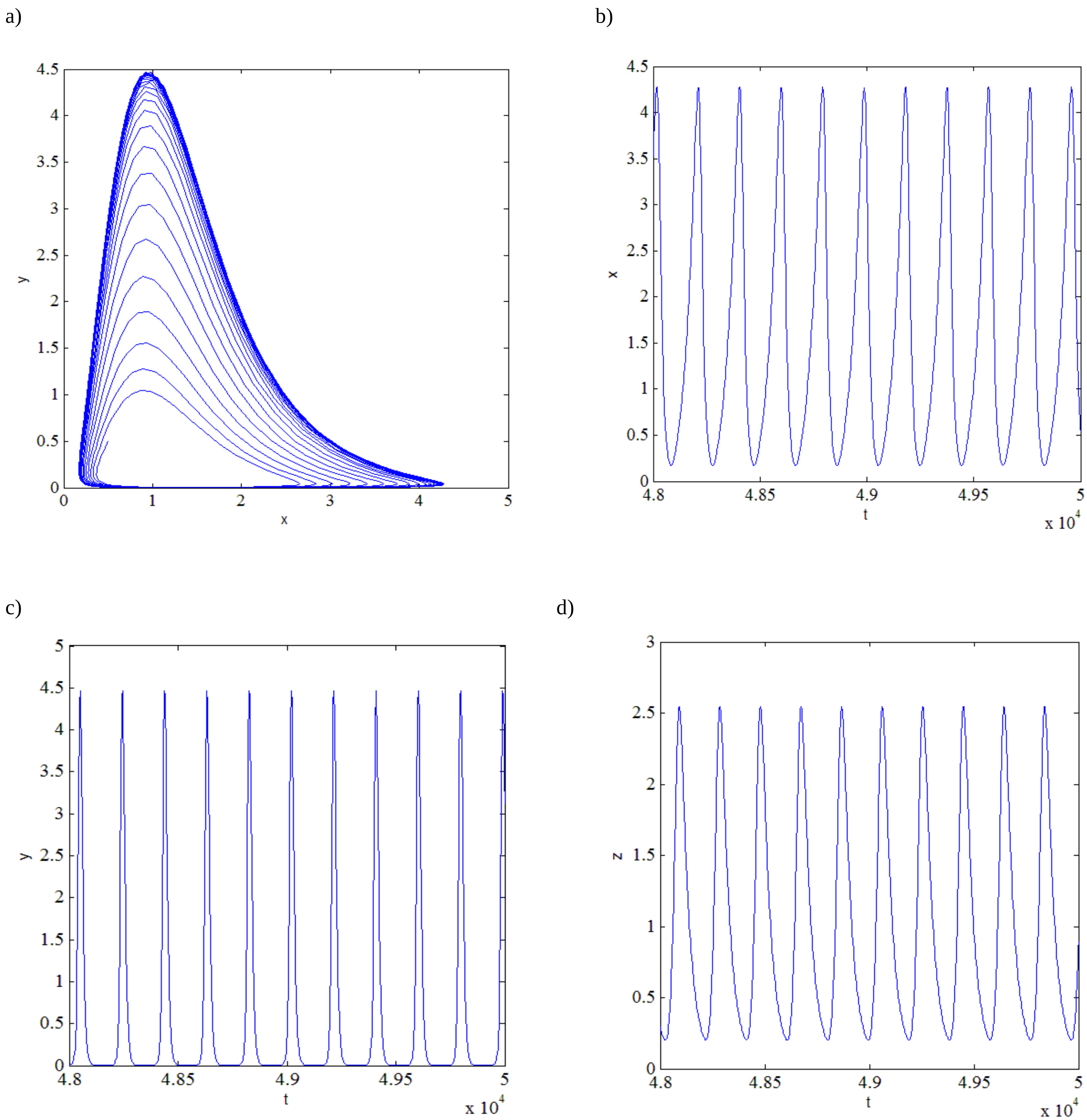

Fig. 4 A computer simulation of the model systems (4)-(6) with $c_1 = 0.008, c_2 = 0.15, c_3 = 0.8, c_4 = 0.5, c_5 = 0.01, c_6 = 0.9, c_7 = 0.02, c_8 = 0.02,$ $c_9 = 0.08,\ k_1 = 0.08,\ k_2 = 0.01,\ k_2 = 0.01,\ k_3 = 3.9,\ k_4 = 0.06,\ k_5 = 0.08,\ k_6 = 0.5,\ d_1 = 0.07, d_2 = 0.145, d_3 = 0.06,\ \varepsilon = 0.95,\ \delta = 0.95,\ x(0) = 0.5,$ $y(0) = 0.5, z(0) = 1.$ (a) The solution trajectory projected onto the (*x*,*y*)-plane. (b) The corresponding time courses of PTH concentration (*x*), (c) active vitamin D concentration (y), and (d) calcium concentration (z), respectively .

A numerical result of the system (4)-(6) is presented in Fig. 5, with parametric values chosen to satisfy the inequalities identified in Case 2. The solution trajectory, shown in Fig. 5a project onto the (x, y)-plane, tends to a stable equilibrium as theoretically predicted. The corresponding time courses of the PTH, active vitamin D, and calcium concentration are as shown in Fig. 5b, 5c, and 5d respectively.

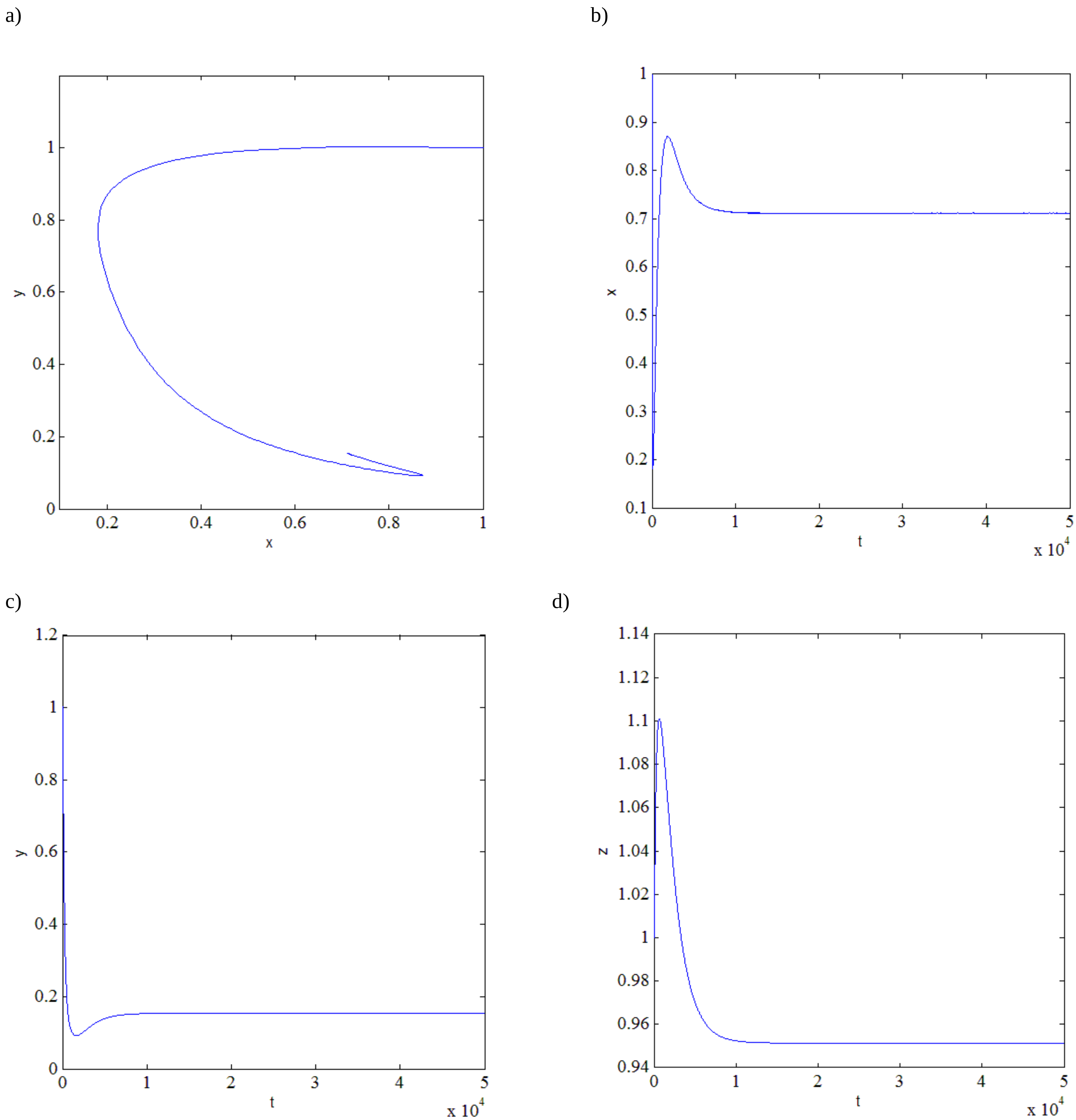

Fig. 5 A computer simulation of the model systems (4)-(6) with $c_1 = 0.008, c_2 = 0.15, c_3 = 0.8, c_4 = 0.9, c_5 = 0.01, c_6 = 0.9, c_7 = 0.02, c_8 = 0.02,$ $c_9 = 0.08,\ k_1 = 0.08,\ k_2 = 0.01,\ k_2 = 0.01,\ k_3 = 3.9,\ k_4 = 0.06,\ k_5 = 0.08,\ k_6 = 0.5,\ d_1 = 0.05, d_2 = 0.145, d_3 = 0.06,\ \varepsilon = 0.95,\ \delta = 0.95,\ x(0) = 0.5,$ $y(0) = 0.5, z(0) = 0.5$. (a) The solution trajectory projected onto the (*x*,*y*)-plane. (b) The corresponding time courses of PTH concentration (*x*), (c) active vitamin D concentration (y), and (d) calcium concentration (z), respectively .

A numerical result of the system (4)-(6) is presented in Fig. 6, with parametric values chosen to satisfy the inequalities identified in Case 3. The solution trajectory, shown in Fig. 6a project onto the (x,y)-plane, tends to a stable equilibrium as theoretically predicted. The corresponding time courses of the PTH, active vitamin D, and calcium concentration are as shown in Fig. 6b, 6c, and 6d respectively.

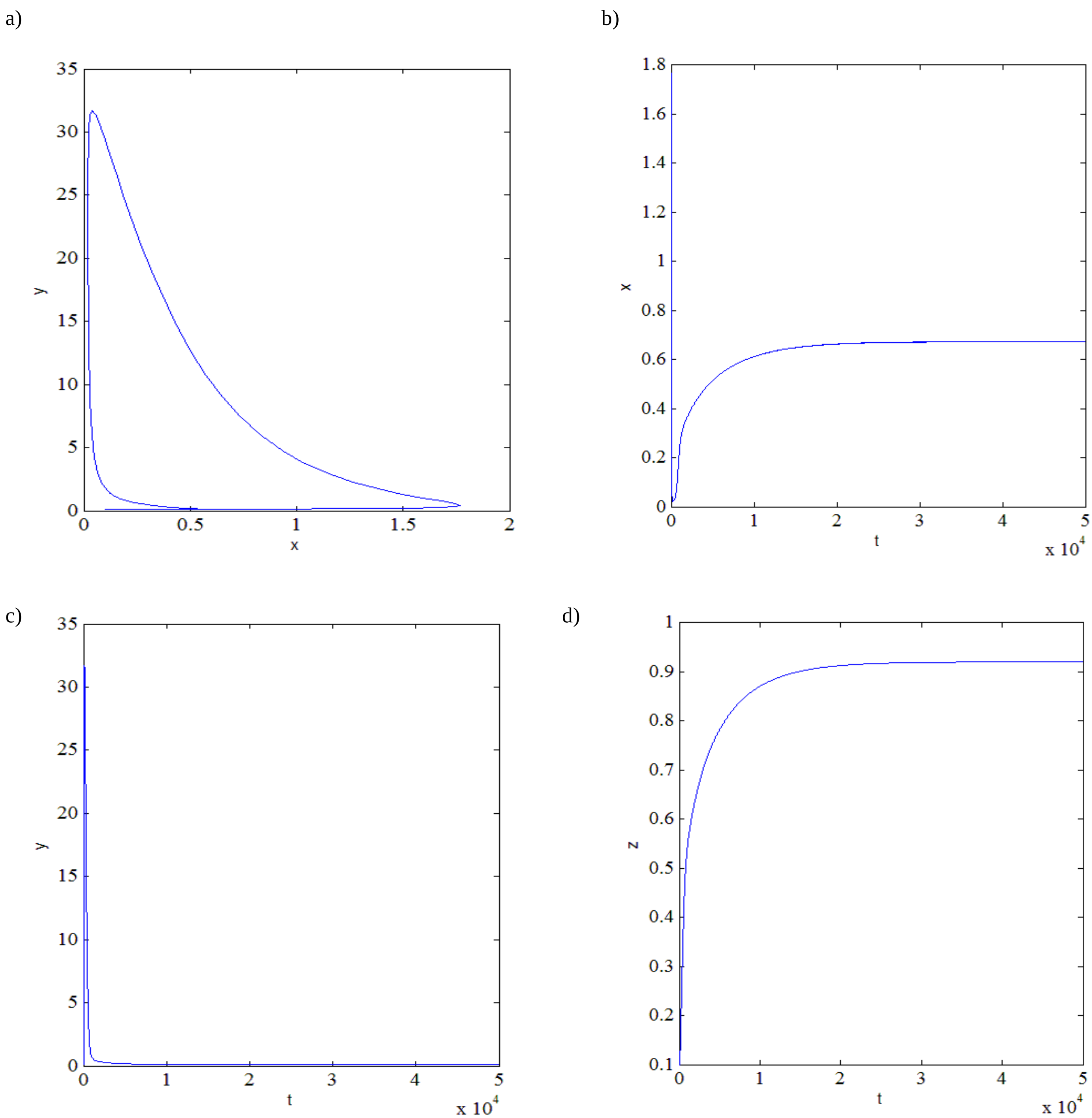

Fig. 6 A computer simulation of the model systems (4)-(6) with $c_1 = 0.008, c_2 = 0.15, c_3 = 0.8, c_4 = 0.5, c_5 = 0.01, c_6 = 0.9, c_7 = 0.02, c_8 = 0.02$, $c_9 = 0.08$, $k_1 = 0.08$, $k_2 = 0.01$, $k_2 = 0.01$, $k_3 = 3.9$, $k_4 = 0.06$, $k_5 = 0.08$, $k_6 = 0.5$, $d_1 = 0.07, d_2 = 0.145, d_3 = 0.06$, $\varepsilon = 0.95$, $\delta = 0.95$, $x(0) = 0.5$, $y(0) = 0.5$, $z(0) = 1$. (a) The solution trajectory projected onto the (*x*,*y*)-plane. (b) The corresponding time courses of PTH concentration (*x*), (c) active vitamin D concentration (y), and (d) calcium concentration (z), respectively .

V. CONCLUSION

A system of nonlinear ordinary differential equations are developed in order to describe calcium homeostasis by focusing on the effects of parathyroid hormone and vitamin D. Geometric singular perturbation is then applied in order to obtain the delineating conditions that differentiate various kinds of dynamic behavior exhibited by the system. In this paper, we present the results in 3 cases. In Case 1, a periodic solution is expected. In Case 2 and 3, a stable equilibrium solution is expected. The well-known Runge-Kutta method which has been used to find an approximation of a solution for the system of ordinary differential equations [13]-[16] is then utilized in order to find an approximation of a solution of our system in each of the three cases. Computer simulations carried out in each case confirm our theoretical predictions. Both theoretical and numerical results show that our system can deduce a periodic behavior which closely resembles to the pulsatile patterns observed clinically in the serum level of parathyroid hormone, vitamin D and calcium [17]-[19].

REFERENCES

[1] H.M. Goodman, *Basic Medical Endocrinology*, 3rd edition, Academic Press, 2003.

[2] S.D. Boden, F.S. Kaplan, “Calcium homeostasis”, *Orthop. Clin. North Am.*, vol.21, no.1, pp. 31-42, 1990.

[3] G.R. Mundy, T.A. Guise, “Hormonal control of calcium homeostasis”, *Clin. Chem*., vol.45, no.8 (B), pp. 1347-1352, 1999.

[4] G. Carmeliet, S.V. Cromphaut, E. Daci, C. Maes, R. Bouillon, “Disorder of calcium homeostasis, *best practice & research clinical endocrinology & metabolism*, vol.17, no.4, pp. 529-546, 2003.

[5] E.M. Brown, “Extracellular Ca2+ sensing, regulation of parathyroid cell function, and role of Ca2+ and other ions as extracellular (first) messengers”, *Physiol. Rev.*, vol.71, pp. 371-411, 1991.

[6] Standing Committee on the Scientific Evaluation of Dietary Reference Intakes, Food and Nutrition Board, Institute of Medicine, *Dietary Reference Intakes: For Calcium, Phosphorus, Magnesium, Vitamin D and Fluoride*, Washington, D.C: National Academy Press, 1997, pp. 250-287.

[7] M.F. Holick, “Vitamin D and bone health”, *J. Nutr.*, vol.126, pp. 1159S-1164S, 1996.

[8] H. Darwish, H.F. DeLuca, “Vitamin D-regulated gene expression”, *Crit. Rev. Eukaryotic Gene Express*, vol.3, pp. 89-116, 1993.

[9] M.F. Holick, “Vitamin D: new horizons for the 21st century”, *Am. J. Clin. Nutr.*, vol.60, pp. 619-630, 1994.

[10] M.F. Holick, *Vitamin D: Photobiology, Metabolism and Clinical Applications, Endocrinology*, 3rd edition, W.B. Saunders, Philadelphia, PA, 1995, pp. 990-1013.

[11] T.J. Kaper, “An introduction to geometric methods and dynamical systems theory for singular perturbation problems. Analyzing multiscale phenomena using singular perturbation methods”, *Proc. Symposia Appl. Math*, vol.56, 1999.

[12] S. Rinaldi, S. Muratori, “A separation condition for the existence of limit cycle in slow-fast systems”, *Appl. Math. Modelling*, vol.15, pp. 312-318, 1991.

[13] W. Sanprasert, U. Chundang and M. Podisuk, “Integration method and Runge-Kutta method”, in *Proc. 15th American Conf. on Applied Mathematics*, WSEAS Press, Houston, USA, 2009, pp. 232.

[14] M. Racila and J.M. Crolet, “Sinupros: Mathematical model of human cortical bone”, in *Proc. 10th WSEAS Inter. Conf. on Mathematics and Computers in Biology and Chemistry*, WSEAS Press, Prague, Czech Republic, 2009, pp. 53.

[15] N. Razali, R. R. Ahmed, M. Darus and A.S. Rambely, “Fifth-order mean Runge-Kutta methods applied to the Lorenz system”, in *Proc. 13th WSEAS Inter. Conf. on Applied Mathematics*, WSEAS Press, Puerto De La Cruz, Tenerife, Spain, 2008, pp. 333.

[16] A. Chirita, R. H. Ene, R.B. Nicolescu and R.I. Carstea, “A numerical simulation of distributed-parameter systems”, in *Proc. 9th WSEAS Inter. Conf. on Mathematic*al Methods and Computational Techniques in Electrical Engineering, WSEAS Press, Arcachon, 2007, pp. 70.

[17] V. Tangpricha, P. Koutkia, S.M. Rieke, T.C. Chen, A.A. Perez, and M.F. Holick, “Fortification of orange juice with vitamin D: a novel approach for enhancing vitamin D nutritional health”, *Am. J. Clin. Nutr.*, vol.77, pp. 1478-1483, 2003.

[18] M.F. Holick, “Sunlight and vitamin D for bone health and prevention of autoimmune diseases, cancers, and cardiovascular disease”, *Am. J. Clin. Nutr.*, vol.80 (suppl), pp. 1678S-1688S, 2004.

[19] K. N. Muse, S. C. Manolagas, L.J. Deftos, N. Alexander, and S.S.C. Yen, “Calcium-regulating hormones across the menstrual cycle”, *J. Clin. Endocrinol. Metab.*, vol.62, no.2, pp.1313-1315, 1986.